TRANSACTIONS
OF TIANJIN UNIVERSITY

2016, 22: 596-602
DOI 10.1007/s12209-016-2726-7

Blind Image Quality Assessment Based on Wavelet Power Spectrum in Perceptual Domain

Lu Pengluo(路朋罗)[1,2], Li Yongchang(李永昌)[3], Jin Longxu(金龙旭)[1],
Han Shuangli(韩双丽)[1]

(1. Changchun Institute of Optics, Fine Mechanics and Physics, Chinese Academy of Sciences, Changchun 130033, China;
2. University of Chinese Academy of Sciences, Beijing 100049, China; 3. DFH Satellite Co. , Ltd, Beijing 100094, China)

Abstract: Blind image quality assessment (BIQA) can assess the perceptual quality of a distorted image without a prior knowledge of its reference image or distortion type. In this paper, a novel BIQA model is developed in wavelet domain. Considering the multi-resolution and band-passing characteristics of discrete wavelet transform (DWT), an improvement over the power spectrum is put forward, i.e., dubbed wavelet power spectrum (WPS) estimation. Then, the concept of directional WPS is applied to simplify the calculation. Moreover, a rotationally symmetric modulation transfer function (MTF) of human visual system (HVS) is integrated as a filter, which makes the metric to be consistent with the human vision perception and more discriminative. Experiments are conducted on the LIVE databases and three other databases, and the results show that the proposed metric is highly correlated with subjective evaluations and it competes well with other state-of-the-art metrics in terms of effectiveness and robustness.

Keywords: blind image quality assessment; human visual system; wavelet power spectrum

Image quality assessment (IQA) metrics have drawn extensive attention because they can automatically predict the perceived image without human's intervention. According to the availability of reference image, studies dealing with image sharpness are classified into three categories: full-reference IQA, reduced-reference IQA, and no-reference/blind IQA (BIQA).

Under most circumstances, the pristine or undistorted information is unavailable for comparison. Therefore, BIQA renders it significantly in practice and enhances its applicability remarkably. BIQA can also be classified into two categories, i.e., spatial domain and transform domain.

In the former case, spatial domain metrics often rely on detecting the variations of image statistical features, such as the spread of edges and texture, gradient, variance, autocorrelation and kurtosis. Overviews of state-of-the-art approaches were introduced in Refs. [1] and [2]. Ferzli and Karam[1] also presented a sharpness assessment by integrating the concept of just noticeable blur (JNB) into a probability summation model. Bahrami and Kot[2] developed a metric called maximum local variation (MLV). Mittal *et al*[3,4] proposed a blind/referenceless image spatial quality evaluator (BRISQUE), which utilizes the natural scene statistic (NSS) of local luminance coefficients; moreover, they established a natural image quality evaluator (NIQE) based on the construction of a "quality aware" collection of statistical features.

In the latter case, transform domain methods are mostly based on the fact that the blur in an image leads to the attenuation of high spatial frequencies. Moorthy and Bovik[5] proposed a distortion identification-based image verity and integrity evaluation (DIIVINE) method, which deploys the NSS of image wavelet coefficients. Saad *et al*[6] developed a blind image integrity notator using discrete cosine transform (DCT) statistics (BLIINDS-II) based on the NSS of block DCT coefficients. Lu *et al* [7] established a model in contourlet domain, which quantifies the variation of nonlinear dependencies between contourlet coefficients to measure the image degradation. Li *et al*[8] presented a general purpose NR-IQA algorithm SHANIA, which develops an NSS model in shearlet do-

Accepted date: 2016-03-09.
Lu Pengluo, born in 1988, female, doctorate student.
Correspondence to Jin Longxu, E-mail: jinlx@ciomp.ac.cn.

main. Liu *et al*[9] derived dubbed CurveletQA that exploits a model of the log-pdf of curvelet coefficients combined with curvelet orientation information. Wavelet-based methods[10-13] were widely used in evaluating the image quality owing to their multi-resolution characteristic. Vu and Chandler[10] presented a fast wavelet-based method for estimating both the global and local fast image sharpness (FISH). Zhao *et al*[11] employed the expectation of wavelet transform coefficients (WTCs) to estimate the image quality.

Spectrum analytic methods[14-16] estimate the image quality through the variation of high frequency component. However, most spectrum analytic methods are based on Fourier transform (FT), which presents a fixed frequency resolution when the type and size of the window are chosen. Conversely, dyadic digital wavelet transform (WT), which is not redundant and invertible[17], provides a representation of the signal on coefficients partly localized in time and frequency. As a consequence, discrete wavelet transform (DWT) is superior to FT when capturing the low- and high-frequency transients of signals.

Based on the fact that a human is the ultimate observer of the imagery system, an incorporation of an appropriate model of human visual system (HVS) would lead to an improvement in the image assessment process. Various models were empirically proposed[18-20]. Based on the feature that WT matches the multi-channel characteristic of HVS, and combined with a band-pass characteristic of contrast sensitivity function, a weighted wavelet power spectrum measure function is derived in this paper.

This paper is organized as follows. In Sections 1 and 2, the details of the proposed algorithm are provided. Section 3 discusses the experimental results and the comparisons with other state-of-the-art BIQAs. Conclusions are presented in Section 4.

1 Algorithm

1.1 FT and DWT

Given a grayscale image $I(x,y)$ of size $M\times N$, FT is formulated as Eq. (1). According to Parseval's theorem, the relationship between signal power and Fourier coefficients is given by Eq. (2). It can be seen that the power spectral density of a signal can be expressed as the FT of its auto-correlation.

$$F(u,v)=\frac{1}{MN}\sum_{x=1}^{M}\sum_{y=1}^{N}I(x,y)\mathrm{e}^{-2\pi\mathrm{i}x\frac{u}{M}}\mathrm{e}^{-2\pi\mathrm{i}y\frac{v}{N}} \tag{1}$$

$$\frac{1}{MN}\sum_{x=1}^{M}\sum_{y=1}^{N}\left|I(x,y)\right|^2=\sum_{u=-\infty}^{+\infty}\sum_{v=-\infty}^{+\infty}\left|F(u,v)\right|^2 \tag{2}$$

The power spectral density in scale (u,v) is:

$$P_{u,v}=\left|F(u,v)\right|^2 \tag{3}$$

The concept of WT is as below:

$$\psi_{a,b}(t)=\frac{1}{\sqrt{a}}\psi\left(\frac{t-b}{a}\right)\qquad a>0,b\in\mathbf{R} \tag{4}$$

where $\psi_{a,b}(t)$ is the shifted and dilated form of the mother wavelet function; a and b are the scaling factor and shift factor, respectively.

DWT is represented as follows:

$$\psi_{m,n}(x)=2^{\frac{-m}{2}}\psi(2^{-m}x-n) \tag{5}$$

Suppose that the space sequence $\{V^k\}$ is satisfied with multiresolution analysis (MRA) in square integrable function space $L^2(\mathbf{R}^2)$. In order to construct a two-dimensional (2D) MRA, the tensor product space of one-dimensional (1D) MRA can be employed. The 2D separable wavelet function can be derived from scaling function $\phi(x)$ and mother wavelet function $\psi(x)$ as follows:

$$\begin{aligned}&\phi(x,y)=\phi(x)\phi(y)\\&\psi^{\mathrm{H}}(x,y)=\psi(x)\phi(y)\\&\psi^{\mathrm{V}}(x,y)=\phi(x)\psi(y)\\&\psi^{\mathrm{D}}(x,y)=\psi(x)\psi(y)\end{aligned} \tag{6}$$

where $\phi(x,y)$ is the relevant scaling function; and $\psi^i(x,y)\{i=\mathrm{H},\mathrm{V},\mathrm{D}\}$ are independent and spatially oriented frequency detailed features in three directions, i.e., horizontally, vertically and diagonally, respectively. The scaling function and the mother wavelet are an orthonormal basis set of $L^2(\mathbf{R}^2)$.

We denote $W_\phi(i,m,j,n)$ and $W_\psi(i,m,j,n)$ as the coefficients of approximated and detailed sub-signals at different DWT levels, respectively:

$$\begin{aligned}W_\phi(i,m,j,n)&=\sum_{x=1}^{M}\sum_{y=1}^{N}I(x,y)\phi_{i,m;j,n}(x,y)\\W_\psi(i,m,j,n)&=\sum_{x=1}^{M}\sum_{y=1}^{N}I(x,y)\psi_{i,m;j,n}(x,y)\end{aligned} \tag{7}$$

1.2 Human visual system

HVS is a complex information management system, which consists of many nerve cells. According to a well-conceived experimental trial-and-error process [18] and the psychophysical spatial frequency threshold measurements on human observers[19], a particular curve is a composite derived from both references, which is a good working representation of the HVS. The curve is modified in Ref. [20]. The rotationally symmetric modulation

transfer function of HVS can be given by:

$$A(r)=(0.31+0.69r)\exp(-0.29r) \tag{8}$$

where the radial frequency r is in cycles per degree of visual angle subtended. The peak of $A(r)$ can be extended from 1 to 9 cycles per degree[20].

2 Proposed method

The proposed method for image sharpness assessment is derived as follows: employ WT to decompose the image; invert the transform, and apply Parseval's theorem to the reconstruction signal; extract the power spectrum of the high frequency information; integrate HVS model with the directional WPS.

2.1 Directional WPS-based HVS

Through the DWT decomposition, an image can be decomposed into the approximation signal and detailed signals at each level. As the scaling function and the mother wavelet are an orthonormal basis set, Parseval's theorem is employed to build the relationship between the power spectrum of the discrete signal and the WTCs. As shown in Eq. (9), the total energy of the signal satisfies the energy conservation theorem and it is equal to the sum of the energy of scale reconstruction signals. The first term on the right side of Eq. (9) represents the average power of the approximated version of decomposed signal, whereas the second term denotes the sum of average power of the detailed version.

$$\frac{1}{MN}\sum_{x=1}^{M}\sum_{y=1}^{N}\left|I(x,y)\right|^2=\frac{1}{MN}\sum_{m}\sum_{n}\left|W_{\phi}(i_0,m,j_0,n)\right|^2+\sum_{i,j=0}^{+\infty}\frac{1}{MN}\sum_{m}\sum_{n}\sum_{\alpha=\{\mathrm{H,V,D}\}}\left|W_{\psi}^{\alpha}(i,m,j,n)\right|^2 \tag{9}$$

To acquire the high frequency information of an image and consider its simplification, the proposed sharpness metric employs the diagonal coefficients of wavelet decompositions, because the diagonal details represent more general properties. Hence, the power spectra of the diagonal coefficients are extracted as follows:

$$p_{i,j}=\frac{1}{MN}\sum_{m=0}^{2^i-1}\sum_{n=0}^{2^j-1}\left|W_{\psi}^{\mathrm{D}}(i,m,j,n)\right|^2 \tag{10}$$

Fig. 1 is a grayscale image. Its different regions in blue windows are selected as subimages, i.e., A1, A2 and A3. Then, their wavelet power spectra are calculated using Eq. (10). For the convenience of comparison, the 2D power spectrum is converted to 1D type. Simultaneously, in order to validate the performance of the proposed method, the power spectra of the subimages are compared with blurred ones, which are derived from the subimages in Fig. 1 by fuzzy processing. As shown in Fig. 2, the change of power spectrum curves caused by blur can be seen obviously.

Fig. 1 Grayscale image

As can be seen from Fig. 2, the wavelet power spectrum method performs well in keeping the invariance of independent scene. The blur of the image in spatial domain leads to the attenuation of high frequency in the frequency domain. Very low spatial frequency information cannot always be sensitive to the image quality changes, as pointed out by Ref. [14]. Thus, for the FFT-based power spectrum, we start calculating from 2% of Nyquist frequency (0.5 cycles/pixel) to avoid the areas of very low frequency. The high spatial frequency information of an image attenuates due to the blur, and it is also easily contaminated by noise. In practice, when $\rho>0.5$, the value of power spectrum is insignificant and only has a negligible effect on the image quality estimation. It is appropriate to select power spectra sum (PSS) in the range of 0.01—0.5 cycles/pixel as sharpness assessment factor.

$$\mathrm{PSSl}=\sum_{\rho=0.01}^{0.5}P_{i,j}/\mu^2 \tag{11}$$

where μ is the mean value of image grayscale, which aims to decrease the influence of luminance changes.

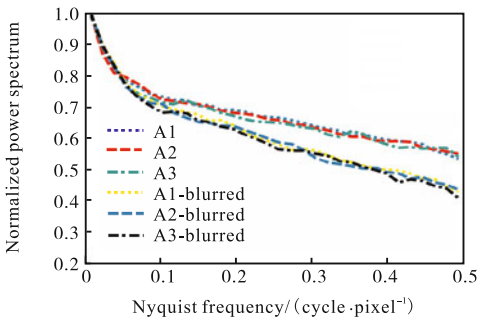

Fig. 2 1D wavelet power spectrum of focusing and defocusing subimages

The square of HVS response function $A(r)$ and WPS are combined as follows to determine a scalar sharpness index, which represents the image's overall sharpness [9]:

$$\mathrm{PSS2} = \sum_{\rho=0.01}^{0.5} A^2(\rho) P_{i,j} / \mu^2 \qquad (12)$$

Fig. 3 shows the variation curves of the proposed method with/without weighting scheme, i.e., Eqs. (11) and (12), for evaluating the image quality through a set of images that are derived by processing an image at various blur levels. The *X*-axis presents the image sequence, while the *Y*-axis stands for the image's normalized sharpness. It can be seen that after weighting, the PSS2 curve exhibits as good monotonicity as PSS1 does. However, the slope of the PSS2 curve increases especially at the focused position, which enhances the sensitivity and accuracy of the proposed sharpness assessment and reduces the misjudgement caused by calculation error effectively. This is because different frequency coefficients make different contributions to visual effect according to the HVS response function. Since we put emphasis on the frequency areas that have more influences on the sharpness assessment, different weights are assigned to wavelet high frequency coefficients owing to the characteristics of HVS.

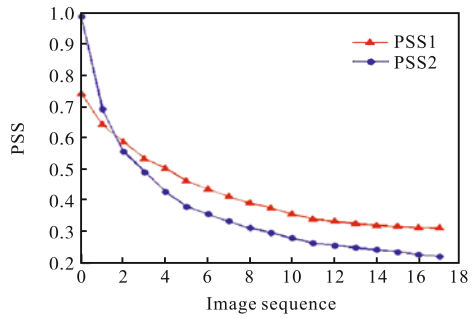

Fig. 3 Variation curves of the proposed method with/without weighting scheme

2.2 Wavelet basis selection

According to the simulation results and the corresponding analysis in Ref.[21], compared with BiorNr.Nd and Morlet which are popular in the wavelet analysis, the merits of Symmlet wavelets include the best orthonormality and compact support, highest vanishing moments, shortest support $2M-1$, approximate symmetry, smallest resulting computational quantity and being able to do DWT. Therefore, Sym2 is selected in our BIQA model.

3 Experimental results and analysis

In this section, experiments are conducted with the LIVE IQA database[22], which contains 779 distorted images derived from 29 reference images by processing them with five distortion types at various levels, i.e., JPEG2000 compression (JP2K), JPEG compression (JPEG), white noise (WN), Gaussian blur (Gblur), and fast-fading (FF) Rayleigh channel distortions. For each image, a difference mean opinion score (DMOS) value is recorded by human observers to describe whether the predicted image quality scores computed by a BIQA model conform to human judgments.

A plot of the predicted DMOS versus the subjective one for each of the data subset is shown in Fig. 4. It can

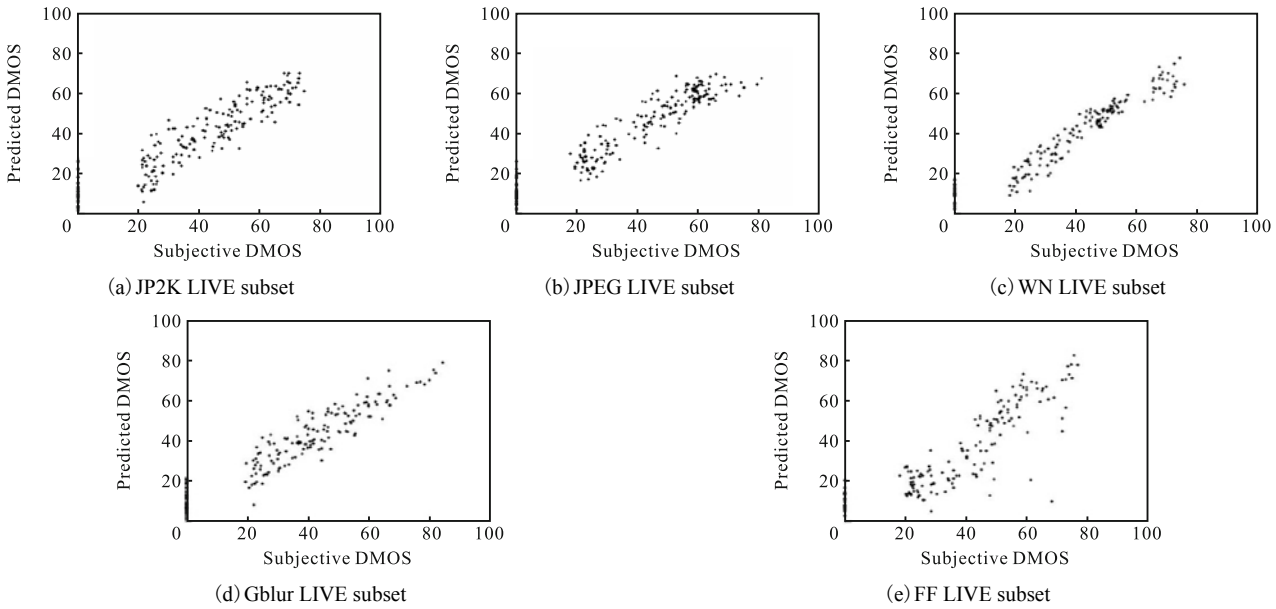

(a) JP2K LIVE subset (b) JPEG LIVE subset (c) WN LIVE subset

(d) Gblur LIVE subset (e) FF LIVE subset

Fig. 4 Predicted versus subjective DMOS

be seen that these scattered plots exhibit good properties: a nearly linear relationship with subjective DMOS, tight clustering, and a roughly uniform spread along the diagonal line. All these properties demonstrate that the proposed method is highly correlated with subjective sharpness evaluations.

To evaluate the performance of predicting subjective ratings of quality quantitatively, two criteria are used: Spearman rank-order correlation coefficient (SROCC) for gauging prediction monotonicity and Pearson linear correlation coefficient (PLCC) for gauging prediction consistency. The larger values for SROCC and PLCC (as close to 1 or −1 as possible) indicate good performance in terms of correlation with HVS. As recommended by the Video Quality Expert Group, when calculating SROCC and PLCC, a nonlinear logistic regression should be built between the predicted scores and the subjective scores due to the nonlinear quality rating of human observers [23]. The logistic regression function is defined as:

$$\mathrm{MOS}_p = \beta_1\left(\frac{1}{2}-\frac{1}{1+\exp\left(\beta_2\left(x-\beta_3\right)\right)}\right)+\beta_4 x+\beta_5 \qquad (13)$$

where x and MOS_p are the predicted scores before and after regression, respectively; β_1 — β_5 are the regression parameters.

We compare our method with seven BIQA methods: NIQE [4], DIIVINE [5], BLIINDS-II [6], BRISQUE [3], Contourlet [7], SHANIA [8] and CurveletQA [9]. In addition, peak signal-to-noise-ratio (PSNR), structural similarity (SSIM), and visual information fidelity (VIF) [24] are also included as benchmarks. To visualize the statistical significance of the comparison, the SROCC and PLCC of the proposed method and other methods are listed in Tab. 1 and Tab. 2, respectively.

Tab. 1 SROCC of different methods on LIVE II database

	JP2K	JPEG	WN	Gblur	FF
PSNR	0.890	0.841	0.985	0.782	0.890
SSIM	0.932	0.903	0.963	0.894	0.941
VIF	0.953	0.913	0.986	0.973	0.965
NIQE	0.917	0.938	0.966	0.934	0.859
BRISQUE	0.918	0.966	0.979	0.948	0.885
DIIVINE	0.912	0.921	0.982	0.937	0.869
Contourlet	0.824	0.562	0.601	0.856	0.823
SHANIA	0.861	0.892	0.958	0.967	0.917
CurveletQA	0.937	0.912	0.988	0.965	0.900
BLIINDS-II	0.946	0.935	0.963	0.934	0.899
Proposed method	0.939	0.954	0.975	0.937	0.878

Tab. 2 PLCC of different methods on LIVE II database

	JP2K	JPEG	WN	Gblur	FF
PSNR	0.896	0.860	0.986	0.783	0.890
SSIM	0.937	0.928	0.970	0.874	0.943
VIF	0.962	0.943	0.984	0.974	0.962
NIQE	0.937	0.956	0.977	0.953	0.913
BRISQUE	0.923	0.973	0.985	0.951	0.903
DIIVINE	0.923	0.935	0.987	0.937	0.892
Contourlet	0.853	0.581	0.958	0.892	0.853
SHANIA	0.914	0.938	0.973	0.979	0.941
CurveletQA	0.946	0.928	0.985	0.969	0.919
BLIINDS-II	0.949	0.951	0.961	0.938	0.901
Proposed method	0.958	0.971	0.963	0.944	0.870

From Tab. 1 and Tab. 2, it can be seen that among all the methods, VIF has the best performance as an FR-IQA method statistically, but it needs the undistorted images as a reference, and so do PSNR and SSIM. In many applications, the reference is not available, which limits the application of FR-IQA, thus BIQA metrics are highly desirable. For the BIQA methods, we list some metrics in both spatial domain and transform domain.

BRISQUE and NIQE operate in spatial domain. Although the proposed method competes well with them, from the perspective of computational complexity, both BRISQUE and NIQE are easily implemented and suitable for real-time applications, while most metrics in transform domain are not.

The performance of the proposed method is also compared with some BIQA methods in transform domain, such as DCT, shearlet and contourlet domain. It is apparent that the proposed metric exhibits significantly superior performance in terms of prediction accuracy and monotonicity. In terms of PLCC, the proposed method achieves correlations of about 0.958 with subjective scores on JP2K subset, and 0.971 on JEPG subset, which are excellent prediction performance for BIQA metric. As for the other types of distortion, the SHANIA and CurveletQA models are better. One drawback of most of these BIQA methods is that a large image dataset is required to get parameters needed. Furthermore, the performance of the methods will be affected more or less when utilizing different train-tests, while the proposed method is a “completely” blind IQA. As a comparison, for the IQA methods, although the proposed method is statistically inferior to the top-performing IQA approaches, it performs quite well on the JP2K and JPEG LIVE subsets, and it is competitive with other methods from the comparison with the other three subsets.

In order to further validate the effectiveness and

universality of the proposed method, experiments were also conducted on four different image quality databases (LIVE, TID2008, CSIQ and IVC). Tab. 3 lists the performance evaluations of SROCC and PLCC of several IQA approaches on the databases. Two best performed metrics are bolded. It can be seen that compared with state-of-the-art IQA metrics, the proposed method achieves encouraging results.

Tab. 3 Performance evaluations of proposed and competing IQA metrics

	LIVE		TID2008		CSIQ		IVC	
	SROCC	PLCC	SROCC	PLCC	SROCC	PLCC	SROCC	PLCC
PSNR	0.829	0.808	0.864	0.834	0.917	0.892	0.695	0.752
NIQE	0.924	0.916	0.736	0.730	0.857	0.870	**0.848**	**0.864**
BRISQUE	**0.943**	**0.933**	**0.873**	**0.852**	**0.936**	**0.914**	0.812	0.831
DIIVINE	0.895	0.912	0.676	0.634	0.832	0.839	0.295	0.299
BLIINDS-Ⅱ	0.924	0.912	**0.874**	**0.859**	0.883	**0.908**	0.593	0.800
Proposed method	**0.942**	**0.968**	0.803	0.788	**0.920**	0.899	**0.896**	**0.907**

In summary, the proposed method gives excellent performance with comparatively larger SROCC and PLCC. The coherence with subjective evaluation validates the efficiency and robustness of the method.

4 Conclusions

In this paper, a BIQA metric based on wavelet power spectrum is proposed, which also takes the response of HVS into account. The proposed method can provide an accurate assessment on the perceived sharpness regardless of the blur types or scene characteristics. The efficiency and robustness of the metric are verified on LIVE databases and three other databases.

References

[1] Ferzli R, Karam L J. A no-reference objective image sharpness metric based on the notion of just noticeable blur (JNB) [J]. *IEEE Transactions on Image Processing*, 2009, 18(4): 717-728.

[2] Bahrami K, Kot A C. A fast approach for no-reference image sharpness assessment based on maximum local variation[J]. *IEEE Signal Processing Letters*, 2014, 21(6): 751-755.

[3] Mittal A, Moorthy A K, Bovik A C. No-reference image quality assessment in the spatial domain[J]. *IEEE Transactions on Image Processing*, 2012, 21(12): 4695-4708.

[4] Mittal A, Soundararajan R, Bovik A C. Making a "Completely Blind" image quality analyzer[J]. *IEEE Signal Processing Letters*, 2013, 20(3): 209-212.

[5] Moorthy A K, Bovik A C. Blind image quality assessment: From natural scene statistics to perceptual quality[J]. *IEEE Transactions on Image Processing*, 2011, 20 (12): 3350-3364.

[6] Saad M A, Bovik A C, Charrier C. Blind image quality assessment: A natural scene statistics approach in the DCT domain[J]. *IEEE Transactions on Image Processing*, 2012, 21(8): 3339-3352.

[7] Lu W, Zeng K, Tao D C *et al*. No-reference image quality assessment in contourlet domain[J]. *Neurocomputing*, 2010, 73(4-6): 784-794.

[8] Li Y M, Po L M, Xu X Y *et al*. No-reference image quality assessment using statistical characterization in the shearlet domain [J]. *Signal Processing*: *Image Communication*, 2014, 29(7): 748-759.

[9] Liu L X, Dong H P, Huang H *et al*. No-reference image quality assessment in curvelet domain [J]. *Signal Processing*: *Image Communication*, 2014, 29(4): 494-505.

[10] Vu P V, Chandler D M. A fast wavelet-based algorithm for global and local image sharpness estimation[J]. *IEEE Signal Processing Letters*, 2012, 19(7): 423-426.

[11] Zhao H J, Fang B, Tang Y Y. A no-reference image sharpness estimation based on expectation of wavelet transform coefficients[C]. In: *International Conference on Image Processing*. Melbourne, Australia, 2013.

[12] Chen Q W, Xu Y, Li C *et al*. An image quality assessment metric based on quaternion wavelet transform[C]. In: *International Conference on Multimedia and Expo Workshops*. San Jose, USA, 2013.

[13] Reenu M, David D, Raj S S A *et al*. Wavelet based sharp features (WASH): An image quality assessment metric based on HVS[C]. In: 2*nd International Conference on Advanced Computing*, *Networking and Security*. Mangalore, India, 2013.

[14] Zhang Y, Jin W Q. A new objective evaluation index to fusion images quality based on power spectrum and HVS

characteristics[C]. In: *Symposium on Photonics and Optoelectronic*. Chengdu, China, 2010.

[15] Qu Y G, Zeng S G, Xia D S. Appraise the CBERS-1 image quality with image information capacity and power spectrum[J]. *Spacecraft Recovery & Remote Sensing*, 2002, 23(2): 40-45(in Chinese).

[16] Zhang Y, An P, Zhang Q W *et al*. A no-reference image quality evaluation based on power spectrum[C]. In: 3*DTV Conference*: *The True Vision-Capture*, *Transmission and Display of* 3*D Video*(3*DTV-CON*). Antalya, Turkey, 2011.

[17] Torrence C, Compo G P. A practical guide to wavelet analysis[J]. *Bulletin of the American Meteorological Society*, 1998, 79(1): 61-78.

[18] Mannos J, Sakrison D J. The effects of a visual fidelity criterion on the encoding of images[J]. *IEEE Transactions on Information Theory*, 1974, IT-20(4): 525-536.

[19] Depalma J J, Lowry E M. Sine-wave response of the visual system. II. Sine-wave and square-wave contrast sensitivity [J]. *Journal of the Optical Society of America*, 1962, 52(3): 328-335.

[20] Nill N. A visual model weighted cosine transform for image compression and quality assessment [J]. *IEEE Transactions on Communications*, 1985, 33(6): 551-557.

[21] Cui H, Song G X. Study of the wavelet basis selections[C]. In: 2006 *International Conference on Computational Intelligence and Security*. Guangzhou, China, 2006.

[22] Sheikh H R, Wang Z, Cormack L *et al*. LIVE Image Quality Assessment Database [EB/OL]. http://live.ese.utexas.edu/research/quality, 2003.

[23] Antkowiak J, Baina T J. *Final Report from the Video Quality Experts Group on the Validation of Objective Models of Video Quality Assessment* [R]. ITU-T Standards Contribution COM, 2000.

[24] Sheikh H R, Bovik A C. Image information and visual quality[J]. *IEEE Transactions on Image Processing*, 2006, 15(2): 430-444.

(Editor: Wu Liyou)